Heat and Mass Transfer Analysis for the MHD Forced Convective Flow of a Nanofluid over a Slendering Stretching Sheet with Radiation in Porous Medium

K. Suneetha[1], G. Venkata Ramana Reddy[2,*], S.M. Ibrahim[3], and Rama Subba Reddy Gorla[4]

[1]*Research Scholar, Department of Mathematics, K. L University Vaddeswaram, Guntur(Dt), 502522, India*

[2]*Department of Mathematics, K L University Vaddeswaram, Guntur(Dt), 502522, India*

[3]*Department of Mathematics, GITAM University, Visakhapatnam, Andhra Pradesh- 530045, India*

[4]*Department of Mechanical Engineering, Cleveland State University, Cleveland, Ohio 44115 USA*

Abstract: Computational analysis of radiative heat and mass transfer of nanofluid over a slendering stretching sheet in porous medium with uneven heat source and slip effects have been carried out in this article. The transformed equations a of the flow model are solved by the Runge-Kutta scheme coupled with shooting method to depict the dimensionless velocity, temperature, and concentration at the boundary layer. Numerical computations are carried out and discussed for skin friction coefficient and local Nusselt number. We found an excellent agreement of the present results with the existed results under some special conditions. It is also found that the heat transfer performance is high in the presence of velocity slip effect. Dimensionless skin-friction coefficient has decreased for increasing magnetic field, power law-index with velocity slip and wall thickness.

Keywords: Nano fluid, Thermal radiation, Porous medium, Slendering stretching sheet, MHD, Heat source.

1. INTRODUCTION

In Recent days one of the principal challenges for the present and future industry is to meet the energy demands of the globe. This Ever-increasing demand is the key factor for the researchers to explore nanoparticles / nanofluids. The enhanced thermal performance of nanofluids / nanoparticles has vital importance in industrial fields such as power generation, micro- manufacturing, transportation, micro-electronics, thermal therapy for cancer treatment, pharmaceutical processes, chemical and metallurgical sectors, etc. In automobiles the application of nanofluids as coolants permit better size as well as positioning of the radiators that require less energy for improving resistance on the road. Ultra-high performance cooling is necessary for many industrial technologies [1-3].

Choi [4-5] was the first to introduce the word nanofluid that represent the fluid in which nanoscale particles (diameter<50 nm) are suspended in the base fluid. With the rapid advances in nanotechnology, many inexpensive combinations of liquid/particles are now available. The base fluids used are usually water, ethylene glycol and oil. Recent research on nanofluids showed that nanoparticles changed the fluid characteristics because thermal conductivity of these particles was higher than convectional fluids. Nanoparticles are of great scientific interest as they are effectively a bridge between bulk materials and atomic or molecular structures.

The study of convective flow, heat and mass transfer in porous media has been an active field of research as it plays a crucial role in diverse applications, such as thermal insulation, extraction of crude oil and chemical catalytic reactors etc. Considerable work has been reported on flow and heat and mass transfer in porous media in [6 – 10].

Magnetohydrodynamics (MHD) boundary-layer flow of nanofluid and heat transfer over a stretching surface has received a lot of attention in the field of several industrial, scientific, and engineering applications in the recent years. The comprehensive references on this topic can be found in some review papers, for example, [11-21] investigated the effects of thermal radiation and magnetic field on the boundary layer flow of a nanofluid over a stretching surface.

The flow in micro/nano systems such as hard disk drive, micro-pump, micro-valve and micronozzles is in slip transition regime, which is characterized by slip boundary at the wall. The liquids exhibiting boundary slip find its applications in technological problems.

*Address correspondence to this author at the Department of Mathematics, K L University Vaddeswaram, Guntur(Dt), 502522, India;
Tel: +918500031137; E-mail: gvrr1976@kluniversity.in

E-ISSN: 2409-5826/19

Therefor, many boundary layer fluid flow problems have been revisited with slip boundary condition and different researchers have made significant contributions. Navier [22] suggested a slip boundary condition in terms of shear stress. Lately or as of late the work of Navier was extended by many authors. GadelHak [23] established the fact that the micro-scale level fluid flow is dominated by fluid surface interaction which belongs to slip flows regime, whereas the momentum equation remains to be Navier-Stokes equation. Slip flow past a stretching surface was analyzed by Andersson [24]. The combined effects of slip and convective boundary conditions on stagnation point flow of CNT suspended nanofluid over a stretching sheet was formulated by Akbar *et al*. [25]. Slip flow effects over MHD forced convective flow over a slendering stretching was studied by Anjali Devi and Prakash [26]. Ramana Reddy *et al*. [27] studied the thermophoresis and Brownian motion effects on MHD nanofluid flow over a slandering stretching sheet in presence of multiple slip effects. Kiran Kumar and Varma [28] examined the MHD boundary layer slip flow of nanofluid through porous medium over a slendering sheet. Sulochana and Sandeep [29] derived the dual solutions analysis on magnetichydrodynamic forced convective flow of a nanofluid over a slendering stretching sheet in the presence of porous medium. Multiple slip and cross diffusion effects on MHD Carreau-Casson fluid over a slendering sheet in presence of non-uniform heat source and sink was proposed by Raju *et al*. [30]. Ramana Reddy *et al*. [31] studied the similar transformations of heat and mass transfer effects on steady MHD free convection dissipative fluid flow past an inclined porous surface with chemical reaction. Ramana Reddy *et al* [32] suggested Lie group analysis of chemical reaction effects on MHD free convection dissipative fluid flow past an inclined porous surface. Venkata Ramana Reddy *et al*. [33] derived Radiation and chemical reaction effects on MHD flow along a moving vertical porous plate. Venkata Ramana Reddy *et al*. [34] established MHD Mixed Convection Oscillatory Flow over a Vertical Surface in a Porous Medium with Chemical Reaction and Thermal Radiation.

To the author's knowledge, no effort has been made still by the researchers to analyze the heat and mass transfer over slendering sheet with heat source or sink and radiation. hence, by exploiting the above-cited studies we made an attempt to fulfill this gap. The considered flow equations are remodeled to a dimensionless form with the aid of suitable transformations. The equations are solved with the support of Runge-Kutta based shooting methods.

2. FORMULATION OF THE PROBLEM

Consider a steady two-dimensional, incompressible, laminar, hydro magnetic flow of a nano fluid over a stretching sheet with non-uniform thickness in porous medium. No-slip and Navier slip conditions are taken in to account. The sheet is along the x-axis direction and y-axis is normal to it as shown in Figure **1**. A variable magnetic field $B(x) = B_0(x+a)^{-(1-n)/2}$, n≠1 is applied to the flow, where B_0 is applied magnetic field strength and a is the physical parameter related to stretching sheet. Magnetic Reynolds number is assumed to be very small so that the induced magnetic field is neglected. A non-uniform permeability $K(x) = k_0(x+a)^{1-n}$, *n≠1* along with the thermal radiation effect is taken into account. Viscous dissipation effect is neglected in this study. It is assumed that the sheet is stretched with the velocity $u_w(x) = u_0(x+a)^n$, n≠1 and the wall temperature $T_w(x) = T_\infty + T_0(x+a)^{(1-n)/2}$, *n≠1*. Since the sheet is non-uniform it is assumed

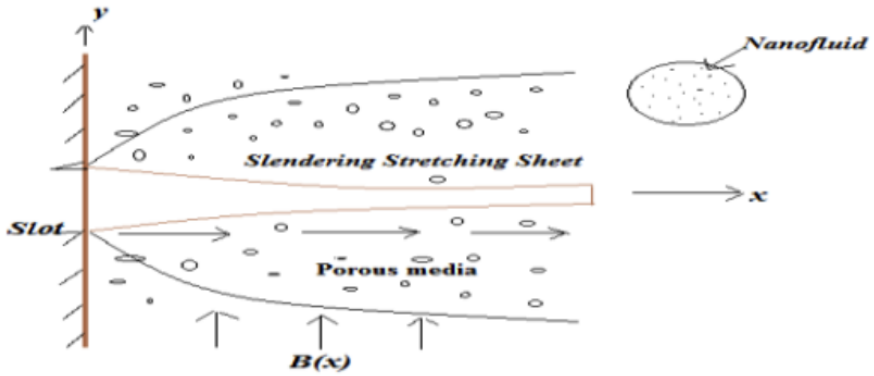

Figure 1: Physical model and coordinate system.

that $y = A(x+a)^{(1-n)/2}$, *n≠1*, where A is the coefficient related to stretching sheet and chosen as a small constant to avoid the external pressure. At m=n=1 the problem refers flat stretching sheet case.

As per the above assumptions the governing boundary layer equations are given as follows: (Devi and Thiyagarajan,[32])

$$\frac{\partial u}{\partial x}+\frac{\partial v}{\partial y}=0 \tag{1}$$

$$u\frac{\partial u}{\partial x}+v\frac{\partial u}{\partial y}=\upsilon_f\frac{\partial^2 u}{\partial y^2}-\frac{\sigma B^2}{\rho_f}u-\frac{\upsilon_f}{K}u \tag{2}$$

$$u\frac{\partial T}{\partial x}+v\frac{\partial T}{\partial y}=\alpha\frac{\partial^2 T}{\partial y^2}-\frac{1}{\rho_f c_p}\frac{\partial q_r}{\partial y}+\tau\left[D_B\left(\frac{\partial C}{\partial y}\frac{\partial T}{\partial y}\right)+\left(\frac{D_T}{T_\infty}\right)\left(\frac{\partial T}{\partial y}\right)^2\right]+\frac{Q_s}{\rho_f c_p}(T-T_\infty) \tag{3}$$

$$u\frac{\partial C}{\partial x}+v\frac{\partial C}{\partial y}=D_m\frac{\partial^2 C}{\partial y^2}+\left(\frac{D_T}{T_\infty}\right)\left(\frac{\partial T}{\partial y}\right)^2 \tag{4}$$

The boundary conditions are as follows

$$u(x,y)=u_w(x)+\delta_1^*\frac{\partial u}{\partial y},\ v(x,y)=0,$$

$$T(x,y)=T_w(x)+\delta_2^*\frac{\partial T}{\partial y},\ C(x,y)=C_w(x)+\delta_3^*\frac{\partial C}{\partial y},$$

at y=0

$$u=0,\ T=T_\infty,\ C=C_\infty \qquad as\ y\to\infty, \tag{5}$$

where *u* and *v* are the velocity components along *x* and *y* directions respectively, ρ_f is the density of the fluid , υ_f is the kinematic viscosity, σ is the electrical conductivity, *T* is the temperature of the fluid, *k* is the thermal conductivity, α is the diffusivity of the nano fluid, $(\rho c_p)_f$ is the specific heat capacitance , Q_s is coefficient of heat source/sink,

δ_1^* is the dimensional velocity slip parameter and δ_1^* is dimensional temperature jump parameter, δ_3^* is dimensional concentration jump parameter, these are given by $\delta_1^*=\left(\frac{2-b}{b}\right)\xi_1(x+a)^{(1-n)/2}$

$\delta_2^*=\left(\frac{2-c}{c}\right)\xi_2(x+a)^{(1-n)/2}$, $\delta_3^*=\left(\frac{2-d}{d}\right)\zeta_3(x+a)^{\frac{1-n}{2}}$,

$\xi_2=\left(\frac{2\lambda}{\lambda+1}\right)\frac{\xi_1}{\mathrm{Pr}}$, $\zeta_3=\left(\frac{2\lambda}{\lambda+1}\right)\frac{\zeta_2}{\mathrm{Pr}}$, hear ξ_1,ξ_2 and ζ_3 are mean free paths and λ is the ratio of specific heats, *b* and *c* respectively indicates Maxwells reflection coefficient and thermal accommodation coefficient.

The radiative heat flux q_r under Rosseland approximation has the form

$$q_r=-\frac{4\sigma^*}{3k^*}\frac{\partial T^4}{\partial y}$$

where σ^* is the Stefan-Boltzman constant and k^* mean absorption coefficient. The temperature differences within the flow are assumed to be sufficiently small such that T^4 may be expressed as a linear function of temperature. Expanding T^4 using Taylor series and neglecting order terms yields

$$T^4\cong 4T_\infty{}^3T-3T_\infty{}^4$$

To convert the governing equations in to set of nonlinear ordinary differential equations we now introducing the following similarity transformation (Devi and Thiyagarajan, [32])

$$\psi(x,y)=\left(\frac{2\upsilon_f u_0}{n+1}\right)^{0.5}(x+a)^{(n+1)/2}f(\eta), \qquad \text{n≠1,}$$

$$\eta=\left(\frac{(n+1)u_0}{2\upsilon_f}\right)^{0.5}(x+a)^{(n-1)/2}y,\ \textit{n≠1}$$

$$\theta(\eta)=(T-T_\infty)/(T_w(x)-T_\infty), \tag{6}$$

where $\psi(x,y)$ is a stream function which satisfies the continuity equations (1) with

$$u=\frac{\partial\psi}{\partial y}\ \text{ and }\ v=-\frac{\partial\psi}{\partial x} \tag{7}$$

Using equations (6)-(7), equations (2) (3) and (4) can be reduced in to the form

$$f'''-\left(\frac{2n}{n+1}\right)f'^2+ff''-(M+K_1)f'=0 \tag{8}$$

$$\frac{1}{\mathrm{Pr}}\left(1+\frac{4}{3}R\right)\theta''-\left(\frac{1-n}{1+n}\right)f'\theta+f\theta'+Nb\theta'\phi'+Nt\theta'^2+Q\theta=0 \tag{9}$$

$$\phi''-Sc\left(\frac{1-n}{1+n}f'\phi-f\phi'\right)+\frac{Nt}{Nb}\theta''=0 \tag{10}$$

With the transformed boundary conditions

$$f(\gamma)=\gamma\left(\frac{1-n}{1+n}\right)\left[1+\delta_1 f''(0)\right],\ f'(\gamma)=\left[1+\delta_1 f''(0)\right]$$

$$\theta(\gamma)=\left[1+\delta_2\theta'(0)\right], \qquad \phi(\gamma)=\left[1+\delta_3\phi'(0)\right],$$

$$f'(\infty)\to 0,\ \theta(\infty)\to 0,\ \phi(\infty)\to 0 \ \text{ n≠1} \tag{11}$$

where $\gamma = A\left(\frac{(n+1)u_0}{2\upsilon_f}\right)^{0.5}$, $\delta_1 = \left(\frac{2-b}{b}\right)\xi_1\left(\frac{(n+1)u_0}{2\upsilon_f}\right)^{0.5}$,

$\delta_2 = \left(\frac{2-c}{c}\right)\xi_2\left(\frac{(n+1)u_0}{2\upsilon_f}\right)^{0.5}$, $\delta_2 = \left(\frac{2-d}{d}\right)\xi_3\left(\frac{(n+1)u_0}{2\upsilon_f}\right)^{0.5}$

Here equations (8) and (10) are nonlinear ordinary differential equations in the domain [γ , δ).

For numerical computation we transformed the domain [γ , δ) in to [0, δ) by defining

$F(\xi) = F(\eta-\gamma) = f(n)$ and $\Theta(\xi) = \Theta(\eta-\gamma) = \theta(\eta)$

Now the similarity equations become

$$F''' - \left(\frac{2n}{n+1}\right)F'^2 + FF'' - (M+K)F' = 0 \quad (12)$$

$$\frac{1}{\Pr}\left(1+\frac{4}{3}R\right)\Theta'' - \left(\frac{1-n}{1+n}\right)F'\Theta + F\Theta' + Nb\Theta'\Phi' + Nt\Theta'^2 + Q\Theta = 0 \quad (13)$$

$$\Phi'' - Sc\left(\frac{1-n}{1+n}F'\Phi - F\Phi'\right) + \frac{Nt}{Nb}\Theta'' = 0 \quad (14)$$

With boundary conditions

$$F(0) = \gamma\left(\frac{1-n}{1+n}\right)\left[1+\delta_1 F''(0)\right], \quad F'(0) = \left[1+\delta_1 F''(0)\right],$$
$$\Theta(0) = \left[1+\delta_2\Theta'(0)\right], \quad \Phi(0) = \left[1+\delta_3\Phi(0)\right],$$
$$F'(\infty)\to 0\ ,\Theta(\infty)\to 0\ ,\Phi(\infty)\to 0\ ,n\neq 1 \quad (15)$$

where the prime indicates the differentiation with respect to ξ . $M = 2\sigma B_0^{\ 2}/\rho_f u_0(1+n)$ is he magnetic field parameter, $K = 2\upsilon_f / k_0 u_0(1+n)$ is the porosity parameter, $\Pr = \upsilon_f/\alpha$ is the Prandtl number, $R = 4\sigma T_\infty^{\ 3}/kk^*$ is the radiation parameter, $Q = \frac{Q_s}{(n+1)\rho_f c_p}$ is the heat source parameter, $Sc = \frac{\upsilon_f}{D_B}$ is the Schmidt number, *n* is the velocity power index parameter, γ is the wall thickness parameter, δ_1 is the non-dimensional velocity slip parameter and δ_2 is the non-dimensional temperature jump parameter,

For engineering interest the shear coefficient or friction factor $\left(C_f\right)$ and local Nusselt number $\left(Nu_x\right)$ and local Sherwood number $\left(Sh_x\right)$ are given by

$$\mathrm{Re}_x^{\ 0.5} C_f = 2\left(\frac{n+1}{2}\right)^{0.5} F''(0), \quad (16)$$

$$\mathrm{Re}_x^{\ -0.5} Nu_x = -\left(\frac{n+1}{2}\right)^{0.5}\Theta'(0), \quad (17)$$

$$\mathrm{Re}_x^{\ -0.5} Sh_x = -\left(\frac{n+1}{2}\right)^{0.5}\Phi'(0) \quad (18)$$

Numerical Solutions

The non-linear ODEs (12) to (14) with corresponding boundary conditions (15) have been solved in the symbolic computation software MATHEMATICA using fourth-fifth order Runge-Kutta – Fehlberg method to obtain the missing values of $F''(0), -\Theta'(0)$ and $-\Phi'(0)$. The present problem involves ten parameters. Therefore, we need to be very selective in the choice of the values of the governing parameters. We apply the far field boundary conditions for similarity variables at a finite value denoted here by $\zeta_{\max}$. We run our bulk computations with the value $\zeta_{\max}$ = 5, which was sufficient to achieve the far field boundary conditions asymptotically for all values of the governing parameters considered.

3. GRAPHICAL OUTCOMES AND DISCUSSION

For numerical solutions we considered the non-dimensional parameter values as M = 1.0, K = 0.5, n = 0.5, Pr = 7.0, Sc = 3.0, R = 0.5, Q = 0.1, γ = 0.2, $0.1 \le \delta_1 \le 0.5$, $\delta_2 = 0.5$ and $\delta_3 = 0.5$ These values are reserved in entire study apart from the variations in consequent figures and tables. To ensure the accuracy of the numerical results we compared the values of $f''(0)$ with the results of Khader and Megahed [32] and Anjali Devi and Prakash [26] in Table **1**. It can be noticed from this table that a worthy agreement between results exist representative graphical/table results for the velocity $\left(F'(0)\right)$, temperature $\left(\Theta(0)\right)$ concentration $\Phi(0)$, friction factor, local Nusselt number and local Sherwood number is presented and also discussed.

The effect of magnetic field parameter on velocity, temperature and concentration profiles of the flow for slip and without slip conditions are displayed in Figures **2**-**4**. From Figure **2** it is noticed that for increasing the magnetic parameter values there is a depreciation in velocity profiles and rise in the temperature and concentration profiles of the flow. It is found that in the presence of slip effect the velocity boundary layer become thin with the increase in the magnetic field

Table 1: Comparison of the Values of $-f''(0)$ when $R = M = \delta_2 = \delta_3 = Q = K = Sc = 0$ and *n* = 0.5

δ_1	γ	Khader and Megahed [32]	Anjali and Prakash [26]	Present
0.0	0.2	0.924828	0.9248281	0.9248282
0.2	0.25	0.733395	0.7333949	0.7333948
0.2	0.5	0.759570	0.7595701	0.7595702

parameter. Since the fluid is electrically conducting, a raise in the value of magnetic field parameter improves the interaction between electric and magnetic field, which causes the Lorentz's force to boost or causes a boost in Lorentz's force. This force works opposite to the flow and reduces the momentum boundary layer thickness and enhances the thermal and concentration boundary layer thickness.

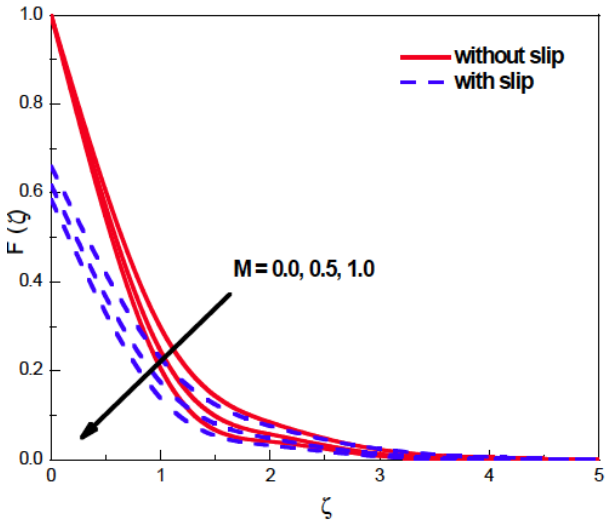

Figure 2: Effects of *M* on velocity profile.

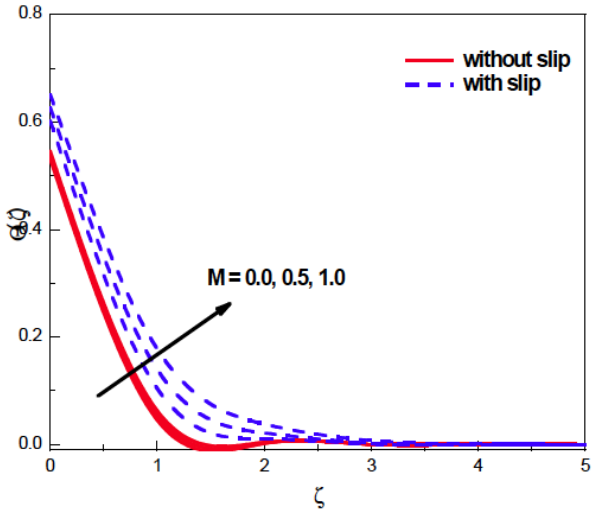

Figure 3: Effects of *M* on temperature profile.

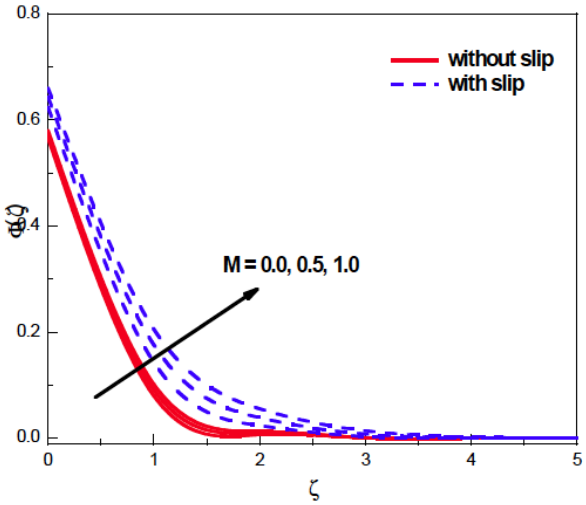

Figure 4: Effects of *M* on concentration profile.

The deviation in velocity, temperature and concentration profiles due to the influence of permeability parameter K is shown in Figures **5**, **6** and **7** for the presence of slip and no-slip conditions. After or with an increase in the porosity parameter, we can observe the similar type of the results as we noticed in the magnetic field parameter case. Since an increase in the porosity parameter widens the holes of porous

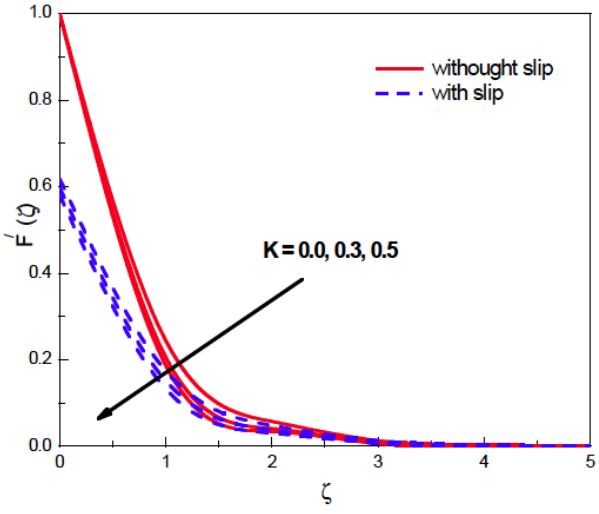

Figure 5: Effects of *K* on velocity profile.

layer, the momentum boundary layer thickness reduces. On not in the order hand a raise in the porosity parameter generates and releases the internal heat energy to the flow. Due to this we observed a rise in the temperature profiles of the flow.

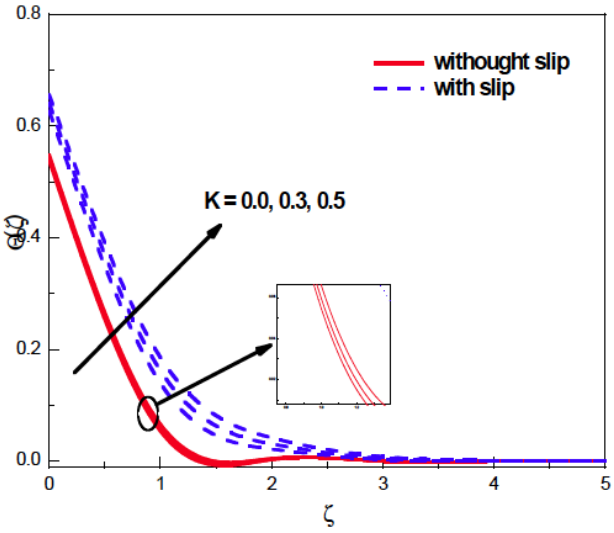

Figure 6: Effects of *K* on temperature profile.

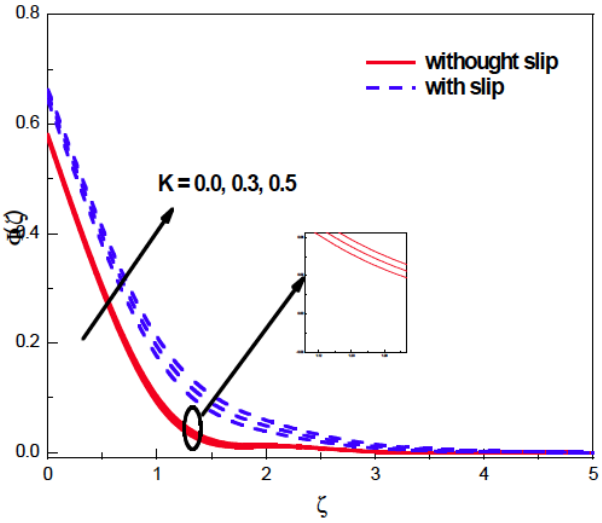

Figure 7: Effects of *K* on concentration profile.

Figure **8** perceives the impact of Prandtl number Pr on the temperature profiles for presence and absence of slip condition cases. It is observed that temperature decreases with an increase of Pr. It is very interesting to find that thickness of the thermal boundary layer is much bigger in presence of slip conditions case compared to the absence of slip condition case.

Figures **9** and **10** respectively present the impact of thermal radiation R and heat generation parameters Q on the temperature profiles of the flow for presence and absence of slip conditions. We have seen from these

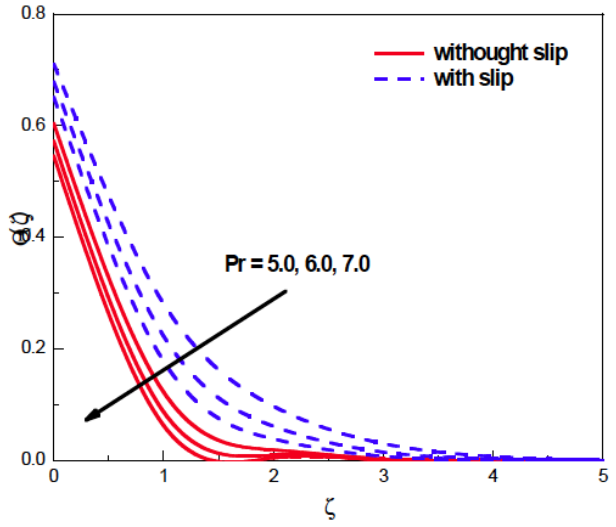

Figure 8: Effects of *Pr* on temperature profile.

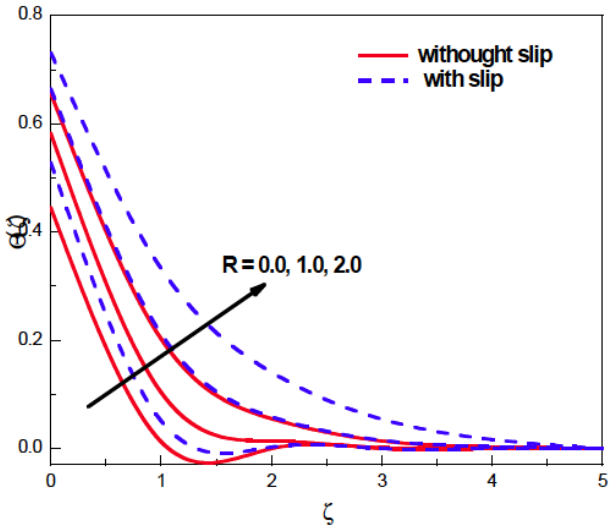

Figure 9: Effects of *R* on velocity profile.

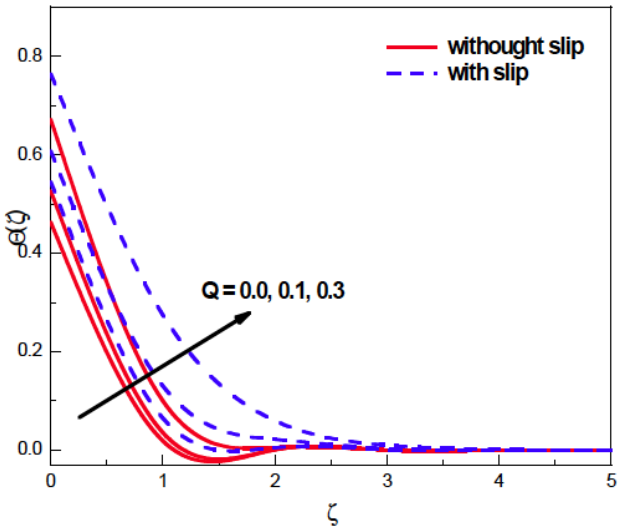

Figure 10: Effects of *Q* on temperature profile.

figures that with the increase in the radiation and heat generation parameters there is a raise in the temperature profiles of the flow. Since increasing the radiation parameter releases the heat energy to the flow.

Figures **11** and **12** shows the variation in the concentration profiles for variation in Schmidt number Sc and concentration jump parameters δ_3 for slip and no-slip cases. We have observed that an as increment in Sc and δ_3 results in decrement in mass diffusivity which in turn decreases concentration boundary layers.

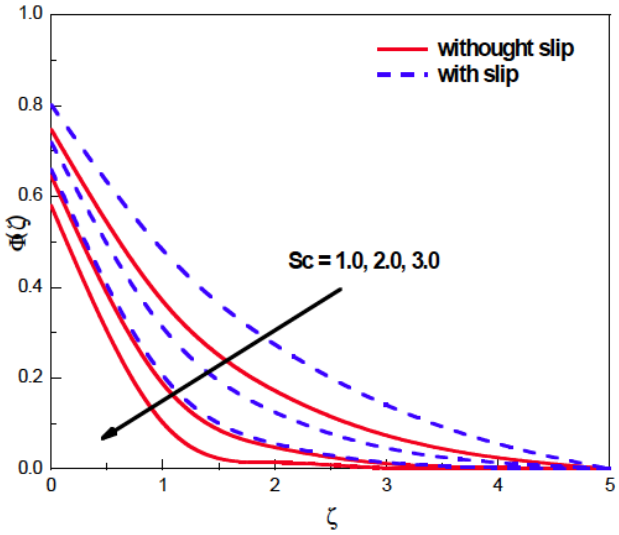

Figure 11: Effects of *Sc* on Concentration profile.

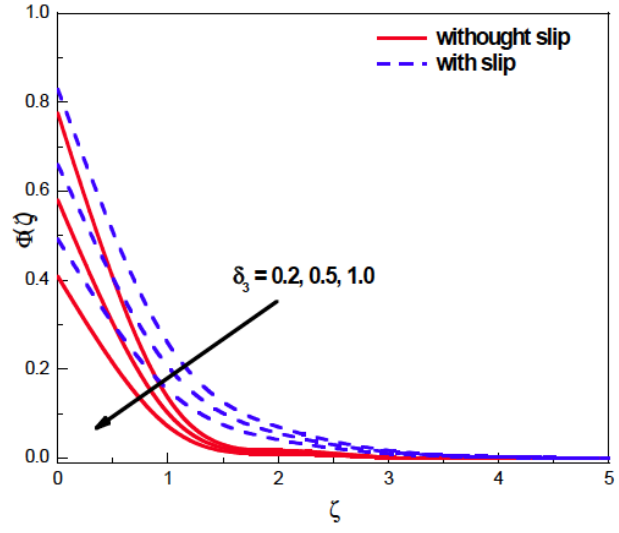

Figure 12: Effects of δ_3 on concentration profile.

Figure **13** displayed the effect of the temperature jump parameter δ_2 on temperature profiles of the flow. It is understood that with an increase in δ_2, we observed depreciation in the temperature profiles of the flow. It is the expected result that an increase in the temperature jump parameter strengthens the thermal accommodation coefficient, which reduces the thermal diffusion towards the flow along with this the thermal boundary layer become thinner with the increase in the temperature jump parameter.

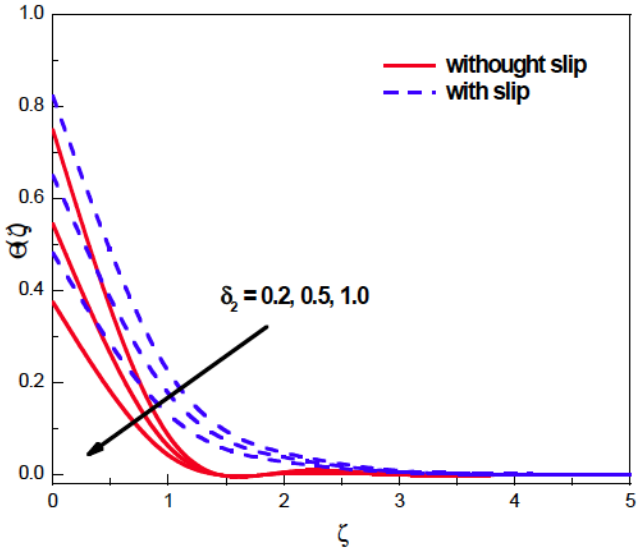

Figure 13: Effects of δ_2 on temperature profile.

The effect of wall thickness parameter γ on velocity, temperature and concentration fields is displayed in Figures **14**, **15** and **16** for with slip and without condition cases. The wall thickness parameter depreciates the velocity, temperature and concentration fields. This may happen due to higher values of wall thickness parameter to improve the thickness of the boundary.

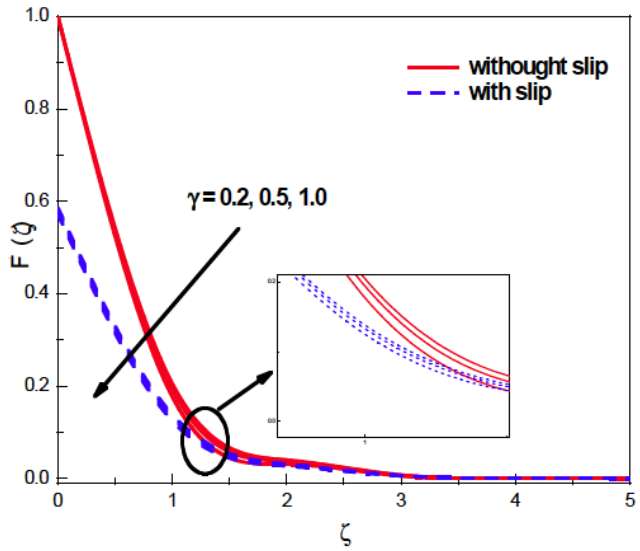

Figure 14: Effects of γ on velocity profile.

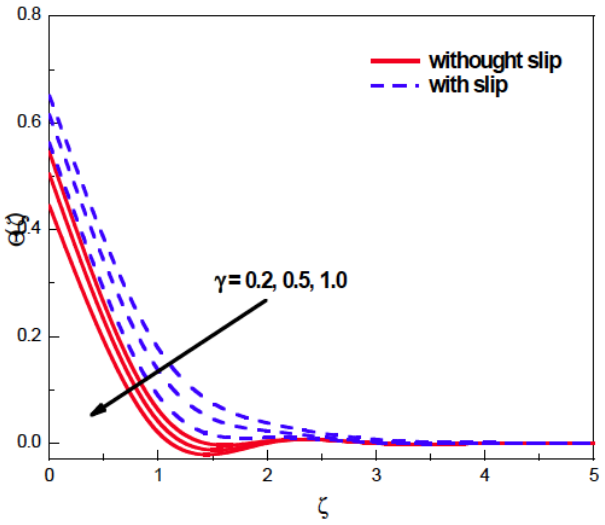

Figure 15: Effects of γ on temperature profile.

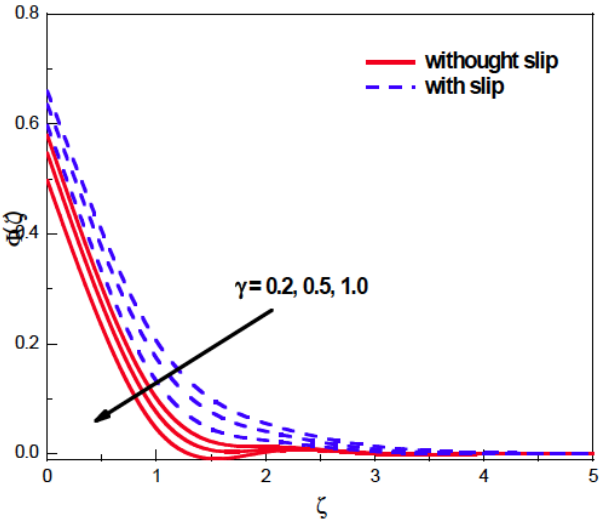

Figure 16: Effects of γ on concentration profile.

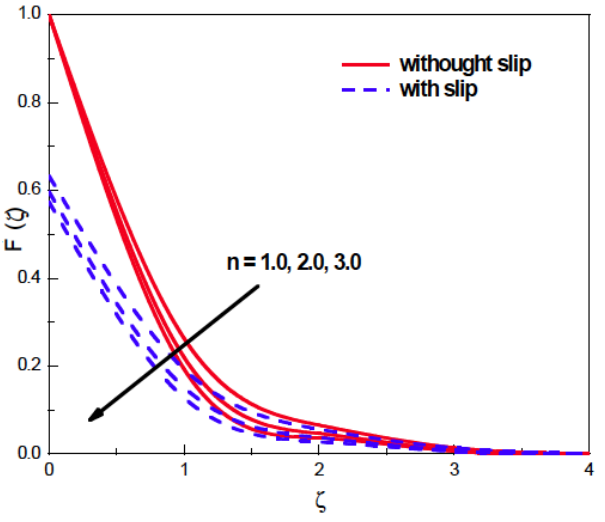

Figure 17: Effects of *n* on velocity profile.

Figures **17**, **18** and **19** portrays the influence of the power law index on velocity, temperature and concentration fields of the flow for slip and no-slip conditions. With the increase in the power law, we noticed a fall in the velocity profiles and a raise in the temperature and concentration profiles. An increase in the power law index reduced the thickness of the sheet. This causes the thermal conductivity and mass conductivity of the flow to improve and reduces the momentum boundary layer thickness.

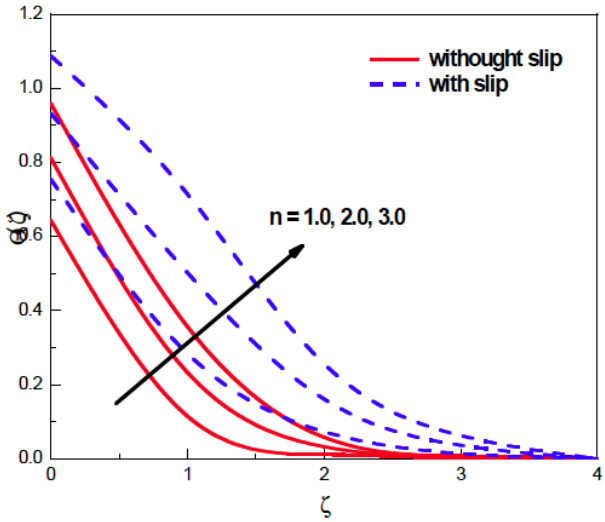

Figure 18: Effects of *n* on temperature profile.

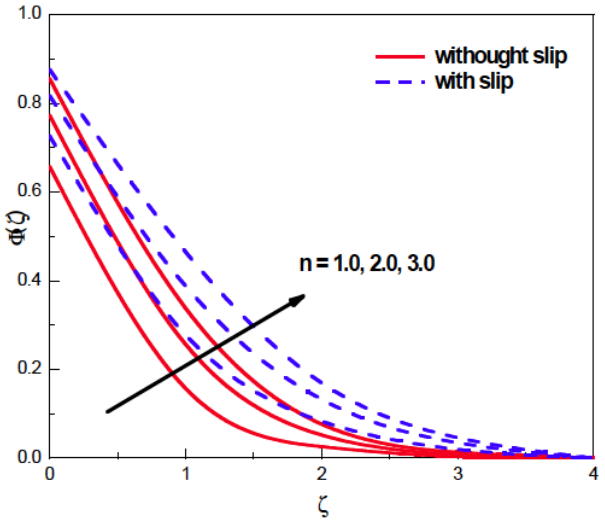

Figure 19: Effects of *n* on concentration profile.

The impact of the thermophoresis *Nt* and Brownian motion parameter *Nb* on the temperature and concentration profiles for slip and no-slip conditions are shown in Figures **20**–**23**. It is observed from these figures that for greater values of both Brownian motion parameter and thermophoresis parameter, temperature and concentration profiles increases.

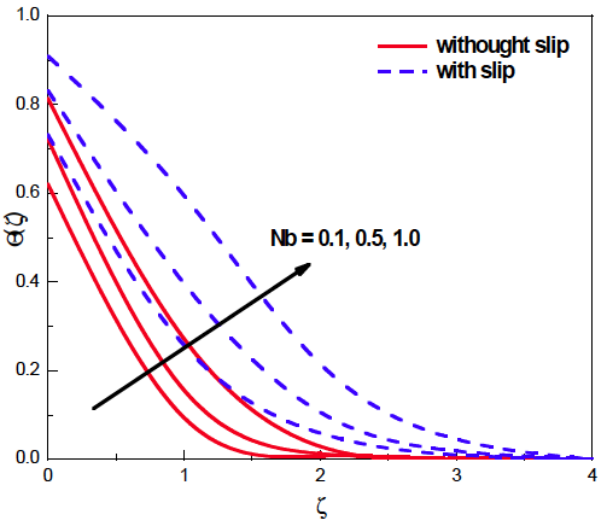

Figure 20: Effects of *Nb* on temperature profile.

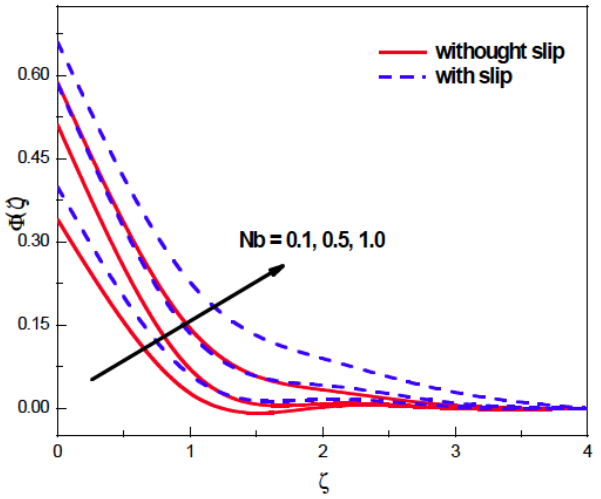

Figure 21: Effects of *Nb* on concentration profile.

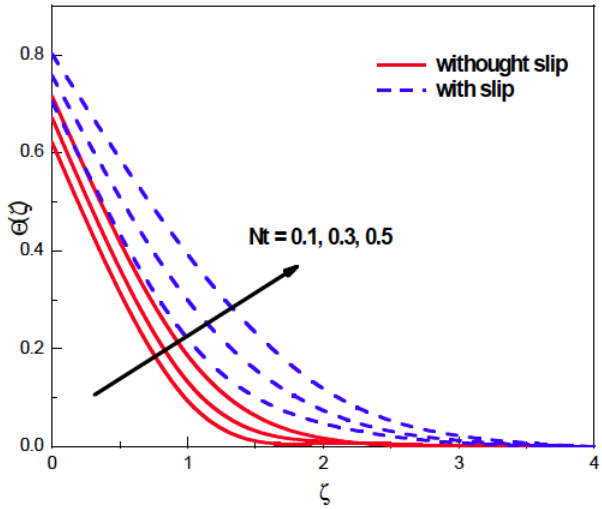

Figure 22: Effects of *Nt* on temperature profile.

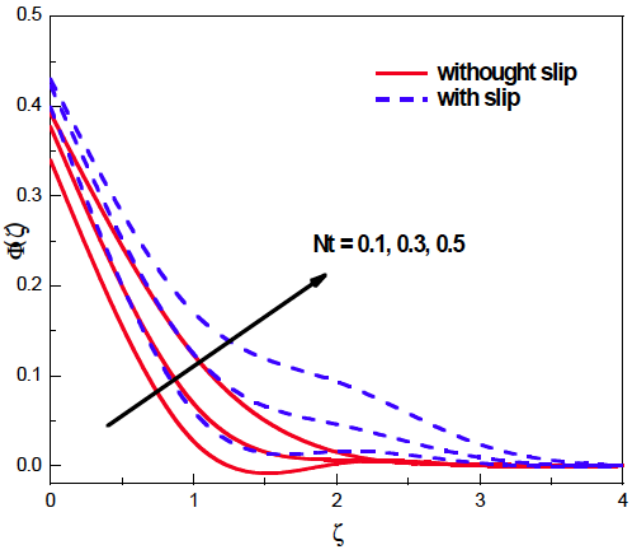

Figure 23: Effects of *Nt* on concentration profile.

The numerical comparisons of, $f''(0)$, $\theta'(0)$ and $-\phi'(0)$ for the different values of *M,K, n, Pr, R, Q,* γ, *Nb, Nt,* δ_2 *and* δ_3 and *Sc* are shown in Table **2** - **3**. The variation in skin-friction coefficient, Nusselt number and Sherwood number for various parameters are investigated through Tables **2** - **3**. The behavior of theses physical parameters is self evident from Tables **2** - **3** and hence, they are not discussed any further to keep brevity.

CONCLUSIONS

Numerical simulation was carried out for dimensionless boundary layer equations of convective heat and mass transfer of a hydromagnetic and nanofluid past over a slendering stretching sheet with radiation and heat source. It is observed from the study that, an increase in the magnetic field reduces the skin-friction factor, local Nusselt number. Increases in power law index depreciate the momentum and enhance the thermal and concentration boundary layer thickness. An increase in the wall thickness the temperature and concentration profiles of the flow to enhance magnetic field have tendency to control the flow. Thermal boundary layer is enriched by magnetic field, velocity power index parameter and dimensionless velocity slip parameter. Thinner thermal boundary layer is obtained for increasing wall thickness, Prandtl number and dimensionless temperature jump parameter. Thinner concentration boundary layer is noticed for increasing Schmidt number.

Table 2: Variation in the Skin-Friction Factor, Local Nusselt Number and Local Sherwood Number at Various non-Dimensional Parameters for slip case

M	*K*	*n*	*Pr*	*R*	*Q*	γ	$F''(0)$	$-\Theta'(0)$	$-\Phi'(0)$
1							-0.834181	0.398791	0.908526
2							-0.927848	0.343296	0.883731
3							-0.997758	0.299088	0.866346
	1						-0.884811	0.369388	0.894937
	2						-0.965079	0.320003	0.874341
	3						-1.02679	0.280207	0.859433
		1					-0.841942	0.182631	0.868854
		2					-0.84935	-0.140451	0.865783
		3					-0.85293	-0.374399	0.897
			7				-0.834181	0.398791	0.908526
			8				-0.834181	0.39602	0.908356
			10				-0.834181	0.38907	0.908713
				1			-0.834181	0.402626	0.909694
				2			-0.834181	0.403818	0.91184
				3			-0.834181	0.403553	0.913226
					0.1		-0.834181	0.402626	0.909694
					0.2		-0.834181	0.300785	0.940196
					0.3		-0.834181	0.16256	0.982128
						0.1	-0.830968	0.464618	0.464618
						0.3	-0.837381	0.497654	1.1037
						0.5	-0.843737	0.53058	1.15836

Table 3: Variation in the Skin-Friction Factor, Local Nusselt Number and Local Sherwood Number at Various Non-Dimensional Parameters for Slip Case

Nb	*Nt*	*Sc*	δ_2	δ_3	$f''(0)$	$-\theta'(0)$	$-\phi'(0)$
0.1					-0.834181	0.522961	1.23753
0.3					-0.834181	0.440607	0.976407
0.5					-0.834181	0.367281	0.860702
	0.1				-0.834181	0.518833	1.089
	0.3				-0.834181	0.445606	1.07351
	0.5				-0.834181	0.381187	1.1183
		3.0			-0.829981	0.379027	0.882156
		5.0			-0.829981	0.385697	1.0599
		10.0			-0.88919	0.510605	1.30746
			0.1		-0.834181	0.570711	1.07166
			0.3		-0.834181	0.523056	1.0723
			0.5		-0.834181	0.481136	1.07357
				0.1	-0.834181	0.425227	1.98953
				0.3	-0.834181	0.461043	1.39492
				0.5	-0.834181	0.481136	1.07357

REFERENCES

[1] Altan T, Oh S, Gegel H (1979) Metal Forming Fundamentals and Applications. American Society of Metals, Metals Park, USA.

[2] Karwe MV, Jaluria Y (1991) Numerical simulation of thermal transport associated with a continuous moving flat sheetin materials processing, ASME J Heat Transfer 113: 612, 619. https://doi.org/10.1115/1.2910609

[3] Kumaran V, Vanav Kumar A, Pop I(2010) Transition of MHD boundary layer flow past a stretching sheet, Commun. Nonlinear Sci Numer Simulat 15: 300-311. https://doi.org/10.1016/j.cnsns.2009.03.027

[4] Choi SUS (1995) Enhancing thermal conductivity of fluids with nanoparticles, The Proceedings of the 1995 ASME International Mechanical Engineering Congress and Exposition. San Francisco, USA.

[5] Choi SUS, Zhang ZG, Yu W, Lockwood FE, Grulke EA (2001) Anomalously thermal conductivity enhancement in nanotube suspensions. Appl Phys Lett 79: 2252-2254. https://doi.org/10.1063/1.1408272

[6] Somers EV (1956) Theoretical considerations of combined thermal and mass transfer from a flat plate ASME. J Appl Mech 23: 295-301

[7] Kliegel JR (1959) Laminar free and forced convection heat and mass transfer from a vertical flat plate, Ph.D. thesis, University of California

[8] Merkin JH (1969) The effects of buoyancy forces on the boundary layer flow over a semi-infinite vertical flat plate in a uniform stream. J Fluid Mech 35: 439-450. https://doi.org/10.1017/S0022112069001212

[9] Lloyd JR, Sparrow EM (1970) Combined free and forced convective flow on vertical surfaces. Int J Heat Mass Transfer 13: 434-438. https://doi.org/10.1016/0017-9310(70)90119-5

[10] Kafoussias NG (1990) Local similarity solution for combined free-forced convective and mass transfer flow past a semi-infinite vertical plate. Int J Energy Res 14: 305-309 https://doi.org/10.1002/er.4440140306

[11] Chamkha AJ, Aly AM (2011) MHD free convection flow of a nanofluid past a vertical plate in the presence of heat generation or absorption effects. Chem Eng Comm 198: 425-441. https://doi.org/10.1080/00986445.2010.520232

[12] Hamad MAA (2011) Analytical solution of natural convection flow of a nanofluid over a linearly stretching sheet inthe presence of magnetic field. Int Commu Heat Mass Transfer 38: 487-492. https://doi.org/10.1016/j.icheatmasstransfer.2010.12.042

[13] Hamad MAA, Pop I, Md Ismail AI (2011) Magnetic field effects on free convection flow of a nanofluid past a verticalsemi-infinite flat plate. Nonlinear Anal Real World Applications 12: 1338-1346. https://doi.org/10.1016/j.nonrwa.2010.09.014

[14] Kandasamy R, Loganathan P, Arasu PP(2011) Scaling group transformation for MHD boundary layer flow of a nanofluidpast a vertical stretching surface in the presence of suction/injection. Nuclear Eng Des 241: 2053-2059. https://doi.org/10.1016/j.nucengdes.2011.04.011

[15] Matin MH, Dehsara M, Abbassi A. (2012) Mixed convection MHD flow of nanofluid over a non-linear stretching sheet with effects of viscous dissipation and variable magnetic field. Mechanika 18: 415-423. https://doi.org/10.5755/j01.mech.18.4.2334

[16] Zeeshan A, Ellahi R, Siddiqui AM, Rahman HU (2012), An investigation of porosity and magnetohydrodynamic flow of non-Newtonian nanofluid in coaxial cylinders. Int J Phys Sci 7: 1353-1361. https://doi.org/10.5897/IJPS11.1739

[17] Khan MS, Mahmud MA, Ferdows M. (2011) Finite difference solution of MHD radiative boundary layer flow of a nanofluid past a stretching sheet. In Proceeding of the International Conference of Mechanical Engineering (ICME '11), BUET, Dhaka, Bangladesh.

[18] Khan MS, Mahmud MA, Ferdows M. (2011)MHD radiative boundary layer flow of a nanofluid past a stretching sheet. In Proceeding of the International Conference of Mechanical Engineering and Renewable Energy (ICMERE '11), CUET, Chittagong, Bangladesh.

[19] F. Mabood, F., SM. Ibrahim, SM, and WA. Khan, WA. Framing the Features of Brownian Motion and Thermophoresis on Radiative Nanofluid Flow Past a Rotating Stretching Sheet with Magneto-hydrodynamics, Results in Physics, vol. 6, pp. 1015-1023, 2016. https://doi.org/10.1016/j.rinp.2016.11.046

[20] F. Mabood, F, SM. Ibrahim, SM., MM. Rashidi, MM, MS. Shadloo, MS, and G. Lorenzini, G., Non-uniform Heat Source/Sink and Soret Effects on MHD Non-Darcian Convective Flow Past a Stretching Sheet in Micropolar Fluid with Radiation, International Journal of Heat and Mass Transfer, vol. 93, pp. 674-682, 2016. https://doi.org/10.1016/j.ijheatmasstransfer.2015.10.014

[21] SM. Ibrahim, SM, and K. Suneetha, K. Heat Source and Chemical Effects on MHD Convection Flow Embedded in a Porous Medium with Soret, Viscous and Joules Dissipation, Ain Shams Engineering Journal, vol. 7, pp. 811-818, 2016. https://doi.org/10.1016/j.asej.2015.12.008

[22] Navier, C. (1827). Sur les lois du movement des liquids. Mem. Acad. R. Sci. Inst. Fr 6, 389-440.

[23] Gadel Hak M, The fluid mechanics of micro devices - the free man scholar lecture. Journal of Fluid Engineering, 121, 5 - 33, 1999. https://doi.org/10.1115/1.2822013

[24] Andersson, H. (2002). Slip flow past a stretching surface. Acta Mechanica 158, 121-125. https://doi.org/10.1007/BF01463174

[25] NS. Akbar, ZH. Khan, S. Nadeem, The combined effects of slip and convective boundary conditions on stagnation-point flow of CNT suspended nano fluid over a stretching sheet, Journal of Molecular Liquids, Vol. 196, pp. 21-25, 2014. https://doi.org/10.1016/j.molliq.2014.03.006

[26] SP Anjali Devi and M Prakash, Slip flow effects over hydromagnetic forced convective flow over a slendering stretching sheet, Journal of Applied Fluid Mechanics, Vol. 9, No. 2, pp. 683-692, 2016. https://doi.org/10.18869/acadpub.jafm.68.225.24064

[27] JV Ramana Reddy, V Sugunamma, and N Sandeep, Thermophoresis and Brownian motion effects on unsteady MHD nanofluid flow over a slendering stretching surface with slip effects, Alexandria Engineering Journal, In Press, 2017. https://doi.org/10.1016/j.aej.2017.02.014

[28] RVMSS Kiran Kumar and SVK Varma, Hydromagnetic boundary layer slip flow of nanofluid through porous medium over a slendering stretching sheet, J. Nanofluids, Vol. 6, pp. 852-861, 2017. https://doi.org/10.1166/jon.2017.1386

[29] C. Sulochana and N. Sandeep, Dual solutions for radiative MHD forced convective flow of a nanofluid over a slendering stretching sheet in porous medium, Journal of Naval Architecture and Marine Engineering 12(2015) 115-124. https://doi.org/10.3329/jname.v12i2.23638

[30] CSK Raju, P. Priyadarshini, SM Ibrahim, Multiple slip and cross diffusion on MHD Carreau-Casson fluid over a slendering sheet with non-uniform heat source/sink, Int. J. Appl. Comput. Math DOI 10.1007/s40819-017-0351-3.

[31] G.V.Ramana Reddy, S.Mohammed Ibrahim and V.S. Bhagavan, Similarity transformations of heat and mass transfer effects on steady MHD free convection dissipative fluid flow past an inclined porous surface with chemical reaction, journal of Naval architecture and marine engineering, December-2014, pp.157-166. https://doi.org/10.3329/jname.v11i2.18313

[32] G. Venkata Ramana Reddy, A Chamkha, "Lie group analysis of chemical reaction effects on MHD free convection dissipative fluid flow past an inclined porous surface", International Journal of Numerical Methods for Heat & Fluid Flow, Vol. 25 (7), pp. - I.F: 1: 399 ,2015. https://doi.org/10.1108/HFF-08-2014-0270

[33] GV. Ramana Reddy, N. Bhaskar Reddy and R.S.R. Gorla, Radiation and chemical reaction effects on MHD flow along a moving vertical porous plate, International Journal of Applied Mechanics and Engineering. Volume 21, Issue 1, Pages 157-168, 2016. https://doi.org/10.1515/ijame-2016-0010

[34] GV. Ramana Reddy, N. Bhaskar Reddy and AJ. Chamkha, MHD Mixed Convection Oscillatory Flow over a Vertical Surface in a Porous Medium with Chemical Reaction and Thermal Radiation, Journal of Applied Fluid Mechanics, Vol. 9, No. 3, 2016. https://doi.org/10.18869/acadpub.jafm.68.228.24021

Received on 1-7-2019 Accepted on 29-8-2019 Published on 13-9-2019

DOI: http://dx.doi.org/10.15377/2409-5826.2019.06.4